Spectrochimica Acta Part A: Molecular and Biomolecular Spectroscopy 105 (2013) 109–124

Contents lists available at SciVerse ScienceDirect

Spectrochimica Acta Part A: Molecular and Biomolecular Spectroscopy

journal homepage: www.elsevier.com/locate/saa

Synthesis and characterization of binary and ternary complexes of Co(II), Ni(II), Cu(II) and Zn(II) ions based on 4-aminotoluene-3-sulfonic acid

Abeer A. Faheim [a,b,*], Safaa N. Abdou [a], Zeinab H. Abd El-Wahab [b]

[a] Chemistry Department, College of Education and Science (Khurma), Taif University, Al-khurma, Taif, Saudi Arabia
[b] Chemistry Department, Faculty of Science (Girl's), Al-Azhar University, P.O. Box 11754, Nasr-City, Cairo, Egypt

HIGHLIGHTS

- ▶ A new Schiff base ligand and its binary and ternary complexes with Co(II), Ni(II), Cu(II) and Zn(II) ions were synthesised.
- ▶ The ligand and its complexes have been characterized by different physicochemical and spectral studies.
- ▶ The antibacterial and antifungal activities have also been performed against different strain of organisms.

GRAPHICAL ABSTRACT

Binary and ternary Co(II), Ni(II), Cu(II) and Zn(II) complexes are reported. The structure of all synthesised compounds was elucidated using different techniques in addition to study their antimicrobial activity.

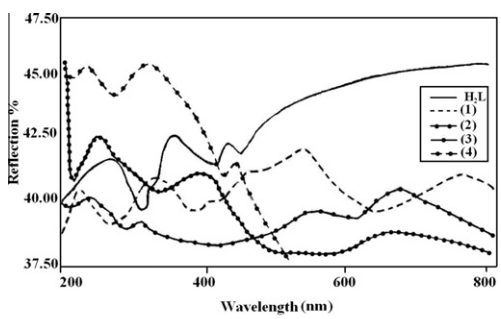

Electronic spectra of Schiff base ligand, H_2L and its Co(II), Ni(II), Cu(II) and Zn(II) binary complexes, (**1-4**) respectively

ARTICLE INFO

Article history:
Received 22 August 2012
Received in revised form 2 December 2012
Accepted 6 December 2012
Available online 14 December 2012

Keywords:
Binary and ternary complexes
Spectroscopic study
Thermal and XRPD analysis
Antimicrobial study

ABSTRACT

Salicylidene (4-aminotoluene-3-sulfonic acid) Schiff base ligand H_2L, and its binary and ternary Co(II), Ni(II), Cu(II) and Zn(II) complexes using 8-hydroxyquinoline (8-HOqu) and 2-aminopyridine (2-Ampy) as secondary ligands have been synthesised and characterized via elemental analysis, spectral data (IR, ^{1}H NMR, mass and solid reflectance), molar conductance, magnetic moment, TG–DSC measurements and XRPD analysis. Correlation of all spectroscopic data suggest that H_2L ligand acts as monoanionic terdentate ligand with ONO sites coordinating to the metal ions via deprotonated phenolic-O, azomethine-N and sulfonate-O while 2-Ampy behaves as a neutral monodentate ligand via amino group-N and 8-HOqu behaves as a monoanionic bidentate ligand through the ring-N and deprotonated phenolic-O. The thermal behavior of these complexes shows that the coordinated water molecules were eliminated from the complexes at relatively higher temperatures than the hydrated water and there are two routes in removal of coordinated water molecules. All complexes have mononuclear structure and the tetrahedral, square planar or an octahedral geometry have been proposed. The ligand and its complexes have been screened for their antimicrobial activity against *Staphylococcus aureus*, *Bacillus subtilis*, *Escherichia coli*, *Salmonella typhimurium*, *Candida albicans* and *Aspergillus fumigatus*. Among the synthesised compounds, the binary and ternary Ni(II) complexes, (**2**, **8** and **10**) and ternary Zn(II) complex, (**12**) were found to be very effective against *Candida albicans* and *Bacillus subtilis* than all other complexes with MICs of 2 and 8 μg/mL, respectively.

* Corresponding author at: Chemistry Department, Faculty of Science (Girl's), Al-Azhar University, P.O. Box 11754, Nasr-City, Cairo, Egypt. Tel.: +20 0163550402.
E-mail address: aafwafy@hotmail.com (A.A. Faheim).

1386-1425/$ - see front matter © 2012 Elsevier B.V. All rights reserved.
http://dx.doi.org/10.1016/j.saa.2012.12.018

Introduction

Benzene sulfonates are used in the production of dyestuffs, tanning agents, catalyst, pesticides, ion exchange resins, plasticizers, pharmaceuticals and chemicals for organic synthesis [1,2]. The p-toluenesulfonic acid is interesting both from the viewpoint of fundamental chemical physics and from a purely practical point of view. Thus, the acid itself finds many useful applications in the manufacture of detergent additives, as a solid electrolyte in oxidizing agents and as a catalyst. Its metal salts, on the other hand, are often used as components of dyed paper and color stabilizers for ink-jet printing sheets [3,4]. Although a survey of the literature reveals that a number of aniline derivatives have been used in preparation of Schiff base ligands, the authors are not aware of any previous publication concerning preparation of Schiff base ligand based on interaction of 4-aminotoluene-3-sulfonic acid with salicylaldehyde as well as its metal complexes; binary and ternary. In view of these finding and in continuation to our previous work on the binary and ternary metal complexes of various Schiff base ligands [5–8], this piece of work has devoted with the aim to synthesize Salicylidene (4-aminotoluene-3-sulfonic acid) Schiff base ligand H_2L, and to examine its complexing ability with Co(II), Ni(II), Cu(II) and Zn(II) ions to form binary and ternary complexes. In preparation of the ternary complexes, 2-aminopyridine (2-Ampy) and 8-hydroxyquinoline (8-OHqu) were used because:

- 2-Aminopyridine and 8-hydroxyquinoline are nitrogen heterocycles and there coordination complexes with (+2) transition metal halides are interest in their packing structures, solid-state reactions, optical, magnetic and redox properties and as model compounds for biological processes [9].
- 2-Aminopyridine serves as useful chelating ligand in a variety of inorganic and organometallic applications. Aminopyridines and their derivatives in most cases act as monodentate ligands which coordinate the metal ions through the nitrogen of the ring as well as amino group, they have wide application in pharmacology and agro-chemistry, serve as a good anesthetic agent and hence are used in the preparation of drugs for certain brain disease [10–12].
- 8-Hydroxyquinoline is a long-known molecule which due to its metal-complexation ability is frequently used for analysis or metal precipitation. Its derivatives are well-known bidentate ligands and are important constituents in a variety of pharmaceutically important compound classes, they are well known for their antifungal, antibacterial and antiamoebic activities [13–16].

Chemistry

The Schiff base ligand Salicylidene (4-aminotoluene-3-sulfonic acid) H_2L, was obtained by means of reaction of 4-Aminotoluene-3-sulfonic acid with salicylaldehyde. The binary complexes (**1**–**4**) were prepared by reacting the metal (II) salts namely $CoCl_2{\cdot}6H_2O$, $NiCl_2{\cdot}6H_2O$, $CuCl_2{\cdot}2H_2O$ and $ZnCl_2$ anhydrous with the ligand H_2L, in 1:1 (M:L) molar ratio. The ternary complexes (**5**–**8**) and (**9**–**12**) were prepared by reacting the same metal (II) salts with the ligand H_2L, in presence of 2-Ampy and 8-OHqu, respectively in a 1:1:1 molar ratio. The structure of the ligand and its metal complexes was confirmed by elemental analysis, spectral data (IR, ^{1}H NMR, mass and solid reflectance), molar conductance, magnetic moment, TG–DSC measurements and XRPD analysis. The synthetic route of the newly Schiff base ligand H_2L, and the proposed structures of the newly obtained metal complexes have been represented in Figs. 1–4.

Pharmacology

Antimicrobial activity

The main aim of the production and synthesis of any antimicrobial compound is to inhibit the causal microbe without any side effects on the patients. In addition, it is worthy to stress here on the basic idea of applying any chemotherapeutic agent which depends essentially on the specific control of only one biological function and not multiple ones. The chemotherapeutic agent affecting only one function has a highly sounding application in the field of treatment by anticancer, since most anticancers used in the present time affect both cancerous diseased cells and healthy ones which in turns affect the general health of the patients. Therefore, there is a real need for having a chemotherapeutic agent which controls only one function [17].

In testing the antimicrobial activity of our compounds more than one test organism was used to increase the chance of detecting antibiotic principles in tested materials. The newly synthesised ligand H_2L, and its binary and ternary complexes were screened in vitro for their antimicrobial activity against different strains of bacteria and fungus. The purpose of the screening program is to

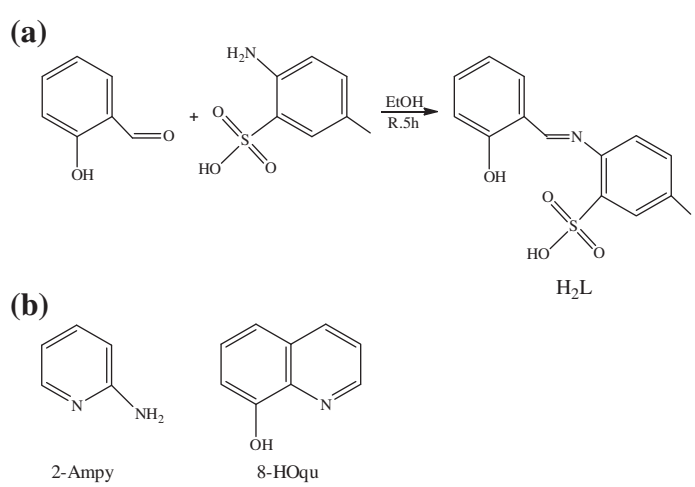

Fig. 1. (a) Pathway of Schiff base ligand, H_2L preparation and (b) ligands used as secondary ligand; 2-Ampy is 2-aminopyridine and 8-HOqu is 8-hydroxyquinoline.

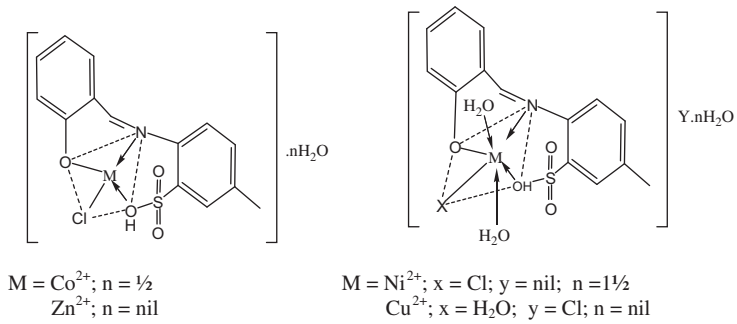

Fig. 2. Proposed structures of the binary complexes; **1–4**.

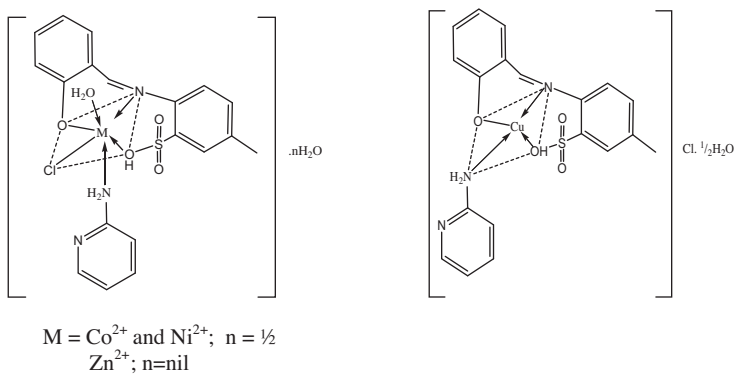

Fig. 3. Proposed structures of the ternary complexes; **5–8** based on 2-aminopyridine.

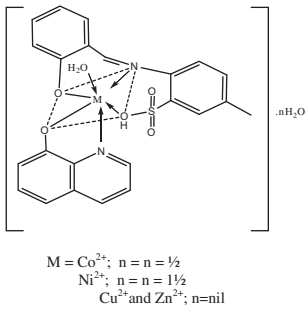

Fig. 4. Proposed structures of the ternary complexes; **9–12** based on 8-hydroxyquinoline.

provide antimicrobial efficiencies of the investigated compounds. The strains include *Staphylococcus aureus* (ATCC 25923) and *Bacillus subtilis* (ATCC 6635) as Gram-positive bacteria; *Escherichia coli* (ATCC 25922) and *Salmonella typhimurium* (ATCC 14028) as Gram-negative bacteria in addition to Yeast; *Candida albicans* (ATCC 10231) and Fungus; *Aspergillus fumigates* using the standardized disk-agar diffusion method [18]. The antibiotics; *Cephalothin* and *Chloramphencol,* were used as standard references for Gram-positive bacteria and Gram-negative bacteria, respectively, while *Cycloheximide* was used as standard reference in the case of yeasts and fungi.

Determination of minimum inhibitory concentration (MIC)

Minimum inhibitory concentration (MIC) is the lowest concentration of an antimicrobial compound that will inhibit the visible growth of a microorganism after overnight incubation [19]. The compounds that showed high or intermediate antimicrobial effect with the agar-disc diffusion assay were selected for minimum inhibitory concentration (MIC) studies through an agar dilution technique [20].

Results and discussion

Condensation of salicylaldehyde with 4-aminotoluene-3-sulfonic acid readily gives rise to Schiff base ligand H_2L, which was easily identified by IR, ^{1}H NMR and mass spectra. The reaction with Co(II), Ni(II), Cu(II) and Zn(II) afford the mononuclear metal complexes in which the microanalytical data as well as metal and chloride estimations, Table 1 are in good agreement with proposed stoichiometries. The reactions follow:

$$H_2L + MCl_2 \cdot xH_2O \rightarrow [M(HL)z]y + HCl + nH_2O$$

M = Co(II); $x = 6H_2O$; z = Cl; $y = ½H_2O$ and $n = 5½$, Ni(II); $x = 6H_2O$; $z = Cl{\cdot}2H_2O$; $y = 1½H_2O$ and $n = 2½$, Cu(II); $x = 2H_2O$; $z = 3H_2O$; y = Cl and n = zero, Zn(II); x = zero; z = Cl; $y = n$ = zero.

$$H_2L + 2\text{-Ampy} + MCl_2 \cdot xH_{2O} \rightarrow [M(HL)(2\text{-Ampy})z]y + HCl + nH_2O$$

M = Co(II); $x = 6H_2O$; $z = Cl{\cdot}H_2O$; $y = ½H_2O$ and $n = 4½$, Ni(II); $x = 6H_2O$; $z = Cl{\cdot}H_2O$; $y = ½H_2O$ and $n = 4½$, Cu(II); $x = 2H_2O$; z = zero; $y = Cl.½H_2O$ and $n = 1½$, Zn(II); x = zero; $z = Cl{\cdot}H_2O$ and n = zero.

$$H_2L + 8\text{-OHqu} + MCl_2 \cdot xH_2O \rightarrow [M(HL)(8\text{-Oqu})(H_2O)]y + nH_2O$$

M = Co(II); $x = 6H_2O$; $y = ½H_2O$ and $n = 4½$, Ni(II); $x = 6H_2O$; $y = 1½H_2O$ and $n = 3½$, Cu(II); $x = 2H_2O$; y = zero and n = 1, Zn(II); $x = y = n$ = zero.

Characterization of Schiff base ligand, H_2L

The structure of the ligand, H_2L was elucidated by elemental analyses, electronic, IR, ^{1}H NMR and mass spectra. The results of

Table 1
Analytical data and some physical properties of the synthesised ligand H_2L, and its binary and ternary complexes.

	Compd. No.[a] empirical formula	Color	Conductance value (Ω^{-1} mol^{-1} cm^2)	Yield %	Elemental analysis, found (calcd.%)					
					C	H	N	S	Cl	M
	H_2L	Yellow	–	85	57.41	4.23	4.53	10.63	–	–
	$C_{14}H_{13}NO_4S$; 291.35				(57.71)	(4.51)	(4.81)	(11.01)		
(1)	[Co(HL)Cl]·½H_2O	Dark	46	88	42.86	2.92	3.13	7.89	9.21	14.75
	$CoC_{14}H_{12}NO_4SCl$.½H_2O; 393.73	Brown			(42.70)	(3.33)	(3.56)	(8.15)	(9.00)	(14.97)
(2)	[Ni(HL)Cl(H_2O)$_2$]·1½H_2O	Dark	42	85	37.46	4.28	2.92	6.78	8.00	12.88
	$NiC_{14}H_{12}NO_4SCl$.3·5H_2O; 447.55	Green			(37.57)	(4.29)	(3.13)	(7.17)	(7.92)	(13.11)
(3)	[Cu(HL)(H_2O)$_3$]Cl	Pale	70	80	38.22	4.42	2.95	7.25	7.97	14.53
	$CuC_{14}H_{12}NO_4SCl$·3H_2O; 443.40	Brown			(37.92)	(4.10)	(3.16)	(7.23)	(8.00)	(14.33)
(4)	[Zn(HL)Cl]	Yellow	10	80	42.72	2.62	3.85	7.82	8.71	16.61
	$ZnC_{14}H_{12}NO_4SCl$; 391.18				(42.98)	(3.10)	(3.58)	(8.20)	(9.06)	(16.72)
(5)	[Co(HL)(2-Ampy)Cl(H_2O)]·½H_2O	Brown	23	85	45.47	4.18	8.15	6.07	6.88	11.86
	$CoC_{19}H_{18}N_3O_4SCl$.1·5H_2O; 505.88				(45.11)	(4.19)	(8.31)	(6.34)	(7.01)	(11.65)
(6)	[Ni(HL)(2-Ampy)Cl(H_2O)]·½H_2O	Green	11	83	45.34	4.13	8.15	5.97	7.21	92.11
	$NiC_{19}H_{18}N_3O_4SCl$.1·5H_2O; 505.64				(45.13)	(4.19)	(8.31)	(6.34)	(7.01)	(11.61)
(7)	[Cu(HL)(2-Ampy)]Cl.½H_2O	Brown	86	85	46.58	3.44	8.35	6.39	6.99	12.51
	$CuC_{19}H_{18}N_3O_4SCl$.0·5H_2O; 492.48				(46.33)	(3.90)	(8.53)	(6.51)	(7.20)	(12.90)
(8)	[Zn(HL)(2-Ampy)Cl(H_2O)]	Yellow	38	79	45.68	3.65	8.12	6.15	7.00	12.82
	$ZnC_{19}H_{18}N_3O_4SCl$·H_2O; 503.33				(45.34)	(4.01)	(8.35)	(6.37)	(7.04)	(12.99)
(9)	[Co(HL)(8-Oqu)(H_2O)]·½	Brown	14	80	53.28	4.23	5.01	5.78	–	11.05
	$H_2OCoC_{23}H_{18}N_2O_5S$.1·5$H_2O$; 520.46				(53.07)	(4.08)	(5.38)	(6.16)		(11.32)
(10)	[Ni(HL)(8-Oqu)(H_2O)]·1½H_2O	Green	31	79	51.37	3.43	5.31	5.68	–	10.74
	$NiC_{23}H_{18}N_2O_5S$.2·5H_2O; 538.24				(51.32)	(3.94)	(5.21)	(5.96)		(10.90)
(11)	[Cu(HL)(8-Oqu)(H_2O)]	Brown	14	75	53.04	3.64	5.96	5.98	–	12.44
	$CuC_{23}H_{18}N_2O_5S$·H_2O; 516.07				(53.53)	(3.91)	(5.43)	(6.21)		(12.31)
(12)	[Zn(HL)(8-Oqu)(H_2O)]	Pale yellow	46	85	53.65	3.58	5.01	5.76	–	12.55
	$ZnC_{23}H_{18}N_2O_5S$·H_2O; 517.91				(53.34)	(3.90)	(5.41)	(6.19)		(12.63)

2-Ampy represent 2-aminopyridine; 8-Oqu represent the deprotonated form of 8-hydroxyquinoline.
1–4 Represent the binary complexes; 5–8 represent the ternary complexes with 2-Ampy and 9–12 represent the ternary complexes with 8-Oqu.
Schiff base ligand, (H_2L) has M.p (°C) 177 and all complexes have M.p > 300.
[a] H_2L represent the Schiff base ligand; HL represent the deprotonated form of Schiff base ligand.

Table 2
Infrared wave numbers (cm^{-1}) and tentative band assignments for the synthesised ligand, (H_2L) and its binary and ternary complexes.

Compd. No.[a]	ν(OH) phenolic/H_2O	ν(C=N)	ν(C–O) phenolic	ν(SO_3)	ν(SO_2–OH)	ν(Ar.ring)	ν(CH_3)	ν(M–O)	ν(M–N)	Other bands[b]
H_2L	3425	1651	1304	1204, 1018	2530	1484, 748	2850	–	–	–
(**1**)	3302	1643	1319	1150, 1034	2561	1466, 733	2855	517	410	–
(**2**)	3294	1597	1373	1157, 1034	2577	1458, 754	2862	524	417	–
(**3**)	3418	1643	1319	1165, 1080	2561	1466, 748	2855	517	424	–
(**4**)	3418	1582	1319	1180, 1034	2492	1466, 733	2886	509	410	–
(**5**)	3734	1566	1400	1150, 1034	2500	1412, 710	2855	517	421′	3186, 1504, 887 (Py.moiety)
(**6**)	3734	1597	1412	1157, 1034	2500	1412, 710	2855	525	455	3256, 1566, 887 (Py.moiety)
(**7**)	3649	1605	1396	1157, 1080	2530	1435, 764	2942	525	440	3225, 1551, 895 (Py.moiety)
(**8**)	3641	1612	1396	1157, 1080	2523	1474, 756	2862	509	448	3256, 1551, 833 (Py.moiety)
(**9**)	3557	1643	1389	1165, 1072	2523	1466, 756	2909	509	440	1551 (Qu.moiety)
(**10**)	3734	1620	1327	1157, 1087	2631	1443, 764	2924	524	448	1535 (Qu.moiety)
(**11**)	3734	1605	1396	1165, 1072	2523	1435, 764	2900	532	456	1551 (Qu.moiety)
(**12**)	3726	1612	1389	1180, 1088	2538	1443, 754	2924	505	448	1535 (Qu.moiety)

[a] Represent the complex number as in Table 1.
[b] Py represent pyridine moiety while Qu represent quinoline moiety.

the elemental analyses (Table 1) are in good agreement with the proposed formula. The formation of ligand is confirmed by the absence of stretching vibration due to amino $\nu(NH_2)$ moiety of 4-aminotoluene-3-sulfonic acid and instead, a strong new band appeared at 1651 cm^{-1} corresponding to the azomethine ν(C=N) group, Table 2 [21,22]. Additionally, IR spectrum of the ligand, H_2L shows a broad band centered at 3425 cm^{-1} assigned to phenolic OH group; ν(OH), [23,24] and a strong band at1304 cm^{-1} assigned to the stretching frequency of the phenolic C—O bond; ν(C—O) [25,26]. Moreover, the ligand spectrum display the characteristic vibrations of S=O associated with the stretching vibration of SO_3 group at 1204 and 1018 cm^{-1} correlate to $\nu(SO_3$ asym stretch) and $\nu(SO_3$ sym stretch), respectively, in addition to a broad band at 2530 cm^{-1} may assigned to $\nu(SO_2$—OH) [27,28]. The bands appearing in the region 1484 and 748 cm^{-1} were usual modes of phenyl ring vibration [29], while that at 2850 cm^{-1} for the CH_3 stretching vibrations of methyl group [30]. The ^{1}HNMR spectrum (300 MHz, DMSO-d$_6$): δ (ppm), of H_2L at ambient temperature, showed signals at 10.68(s, 1H, OH) and 10.23 (s, 1H, SO_3H) as was confirmed by deuterium exchange when D_2O was added to d$_6$-DMSO solution [22,31] in addition to 9.32 (s, 1H, CH=N), 6.92–7.63 (m, 7H, ArH), and 2.36 (s, 3H, CH_3) [32–34]. The mass spectrum of the ligand (Fig. 5) showed its molecular ion peak at m/e = 291.00 with abundance 19.54%, confirming its formula weight = 291.35. The interpretation of its fragmentation is shown in Fig. 6. The electronic spectrum of the free ligand, (Fig. 7) showed three absorption bands in the 438–246 nm, (22,831–40,650 cm^{-1}) region. The two absorption bands at 246 and 358 nm (40,650 and 27,933 cm^{-1}) are practically identical and can be attributed to π–π^* transitions in the benzene/azomethine (C=N) groups. The absorption band observed at 438 nm (22,831 cm^{-1}) is most probably due to the transition of n–π^* of azomethine group [35,36].

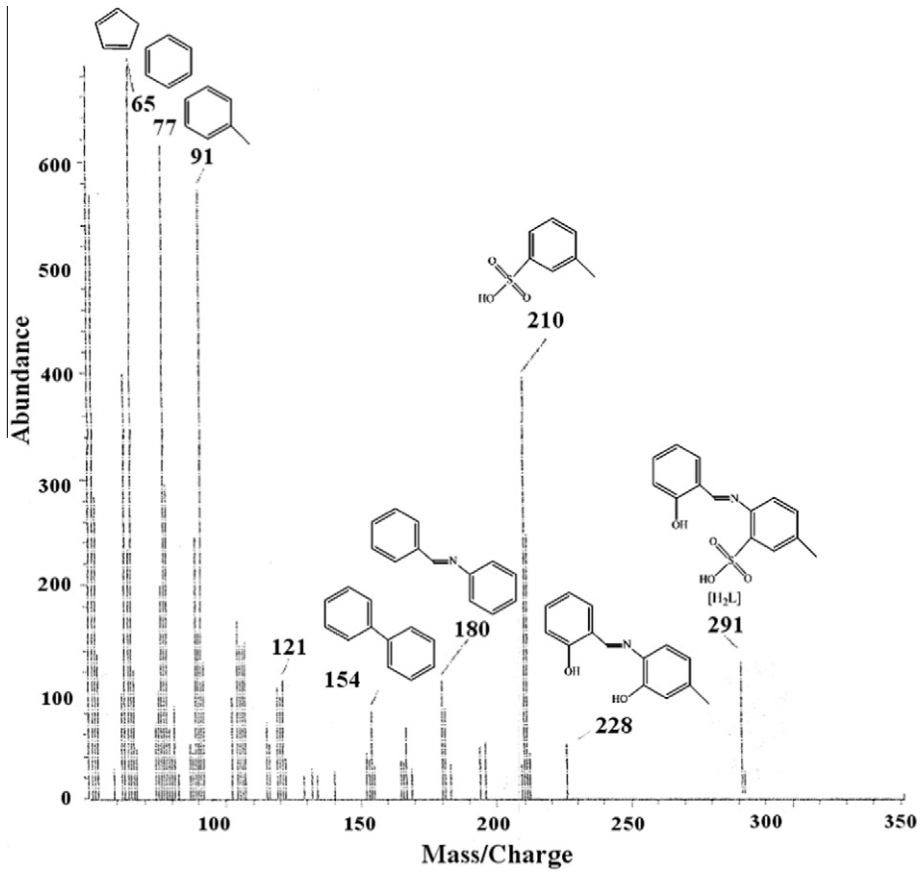

Fig. 5. Mass spectrum of the Schiff base ligand, H_2L.

Characterization of the metal complexes

Infrared spectroscopy

The main IR characteristic stretching frequencies of the ligand and its binary and ternary complexes, (**1**–**12**) along with their proposed assignments are given in Table 2. The determination of the coordinating atoms is made on the basis of the comparison of the IR spectra of the ligand and its complexes. The IR spectra of all complexes, (**1**–**12**) show a shift of the ν(C═N) to lower frequency by 8–85 cm^{-1} compared with the free ligand band at 1651 cm^{-1}.This shift indicates coordination of the azomethine group to the metal ions. In the far IR spectra of all the complexes, the non-ligand bands observed at 456–410 cm^{-1} region assigned to ν(M—N) stretch [37]. The disappearance of the free ligand ν(OH) band around 3425 cm^{-1} in the spectra of all complexes indicating deprotonation of organic ligand prior to coordination. On the other hand, the ν(C—O), which occur at 1304 cm^{-1} for the ligand, was moved to higher frequencies, 1412–1319 cm^{-1} after complexation, this shift confirms the participation of phenolic oxygen of the ligand in C—O—M bond formation [38]. Conclusive evidence regarding the bonding of oxygen to the metal ions is provided by the occurrence of bands at 532–505 cm^{-1} region due to ν (M—O) [39]. Moreover, the characteristic vibrations of S═O associated with the stretching vibration of SO_3 group shift to 1180–1150, 1088–1034 and 2631–2492 cm^{-1}, respectively, confirming its involvement in coordination [40]. IR spectra of the ternary complexes based on 2-Ampy, **(5**–**8)** showed three new bands at 3256–3186, 1566–1504 and 895–833 cm^{-1} assigned to the coordinated NH_2 group, skeletal vibration of pyridine ring and pyridine ring breathing mode, respectively, whereas, the ternary complexes based on 8-OHqu, **(9**–**12)** show new bands in the range 1551–1535 cm^{-1}, due to the azomethine group of the quinoline ring in addition to the absence of band due to the OH group of the hydroxyquinoline indicating that 2-Ampy and 8-HOqu act as neutral monodentate and monoanionic bidentate ligands, respectively [5,7]. Finally, the assignment of the nature of water molecules associated with the complex formation under study was much more complicated as ligands vibrations interfere in this region. The thermal data confirms the nature of water molecule to be lattice/coordinated. The thermal study will be discussed in detailed manner later.

^{1}H NMR spectroscopy

The ^{1}HNMR spectral data of the diamagnetic Zn(II) complexes (**4**, **8** and **12**) were analyzed in comparison of the spectrum of the free ligand, H_2L. The disappearance of the signal due to phenolic (OH) proton in all Zn(II) complexes referring to its involvement in coordinating with the metal ions after deprotonation while the appearance of the signal assigned to sulfonic proton at 10.53–10.31 ppm in the spectra of all complexes supports the involvement of sulfonic group in coordination with the metal ions [18]. The coordination of the azomethine nitrogen is inferred by the downfield shifting of the —CH═N— proton signal from 9.32 ppm in the free ligand to 9.76–9.54 ppm in all complexes. Moreover, the signal due to —CH_3 protons appears at δ 2.37–2.55 ppm in metal complexes. In the spectrum of Zn(II) complex **4**, the aromatic protons were observed as a multiplet at 6.94–7.91 ppm while the mixed 2-Amp complex **8**, showed a multiplet at 6.99–8.05 ppm assigned to aromatic and pyridine protons in addition to a broad singlet at 5.01 ppm is indicative of coordinated NH_2 protons [29], however, the mixed 8-OHqu complex **12**, showed a multiplet at 6.97–8.25 ppm assigned to aromatic and quinoline protons and

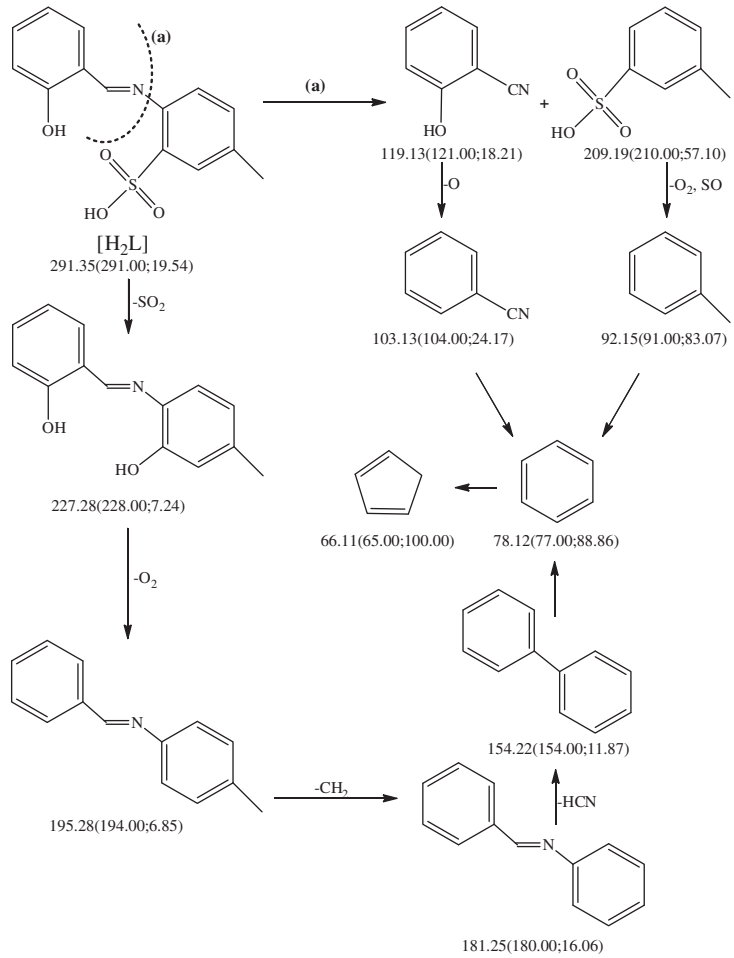

Fig. 6. Mass fragmentation pattern of Schiff base ligand, H_2L where the values under each fragment denoted as calculated (found; intensity).

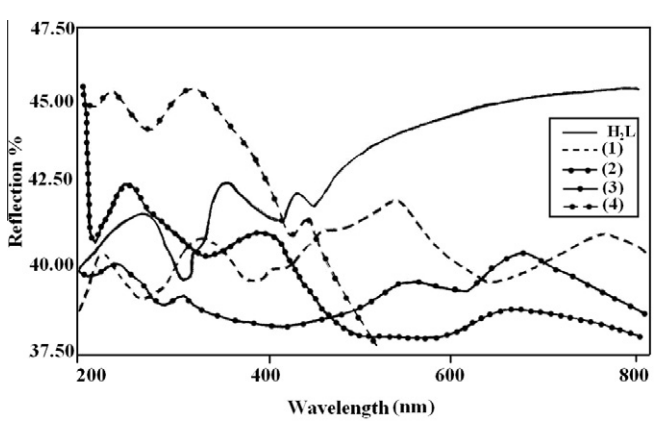

Fig. 7. Electronic spectra of Schiff base ligand, H_2L and its Co(II), Ni(II), Cu(II) and Zn(II) binary complexes, (**1**–**4**) respectively.

do not show a signal due to the OH group of 8-OHqu which indicates the deprotonation of this group during the formation of complexes.

Conductivity measurements

The molar conductance values of the metal complexes in DMF (10^{-3} M solution) were measured at room temperature and the results are listed in Table 1. It is concluded from the results that the metal complexes, **1**, **2**, **4**–**6** and **8**–**12** were found to have molar conductance values in the range from 10 to 46 Ω^{-1} cm^2 mol^{-1} which indicates that they are non electrolytic in nature and there is no counter ion present outside their coordination sphere [41]. On the other hand, the molar conductivity values of complexes, **3** and **7** were found to have molar conductance values 70 and 86 Ω^{-1} cm^2 mol^{-1}, respectively which indicates the ionic nature of these complexes and the type of electrolyte being 1:1 [42].

Magnetic susceptibility measurements

The magnetic measurements of the metal complexes, Table 3 were carried out at room temperature according to the Gauy method. Co(II) complexes, d^7, **1**, **5** and **9** have μ_{eff} values of 4.85–4.65 B.M., corresponding to three unpaired electrons but higher than the spin-only value (3.87) due to the orbital angular momentum contribution in a d^7 system [5]. The magnetic moment values of the Ni(II) complexes, d^8, **2**, **6** and **10** lie in the range 3.01–2.94 B.M. corresponding to two unpaired electrons (the normal expected range for octahedral Ni(II) complexes μ_{eff} = 2.8–3.3 BM) [43]. The magnetic moment of Cu(II) complexes, d^9, **3**, **7** and **11** are in the range 1.96–1.87 corresponding to one unpaired electron [44]. Zn(II) complexes, d^{10}, **4**, **8** and **12** are found to be diamagnetic in nature [45].

Electronic spectra

The electronic reflectance spectra of the ligand and its complexes (**1**–**12**) have been recorded in the 800–200 nm range. Upon complexation with metal ions, the absorption bands attributed to

Table 3
The magnetic properties of metal complexes.

Complex no.[a]	$\mu_{eff.}$[b]	μ_{SO}[c]	No. of unpaired electrons	Hybrid orbitals	Suggested structure
(**1**)	4.65	3.87	3	Sp^3	Tetrahedral
(**2**)	2.99	2.83	2	sp^3d^2	Octahedral
(**3**)	1.96	1.73	1	sp^3d	Octahedral
(**5**)	4.77	3.87	3	sp^3d	Octahedral
(**6**)	2.94	2.83	2	sp^3d	Octahedral
(**7**)	1.87	1.73	1	dsp^2	Square planar
(**9**)	4.85	3.87	3	sp^3d	Octahedral
(**10**)	3.01	2.83	2	sp^3d	Octahedral
(**11**)	1.94	1.73	1	sp^3d	Octahedral

[a] The complexes **4**, **8** and **12** are not cited because they are diamagnetic Zn(II) complexes.
[b] μ_{eff} is an experimental effective magnetic moment calculated.
[c] μ_{so} is spin – only magnetic moment = $[n(n+2)]^{½}$.

π–π* and n–π* transitions were found to be shifted to lower or higher energy regions compared to the free ligand, in addition to appearance of new bands at longer wavelength may be assigned to LMCT/d–d transitions. This generally confirms that the ligand interacts with the metal ion, and the metal ion environments are different leading to the formation of different geometrical types of complexes. Fig. 7 shows electronic spectra of free ligand, H_2L and its Co(II), Ni(II), Cu(II) and Zn(II), binary complexes, (**1**–**4**), respectively as representative example.

The electronic spectrum of Co(II) complex **1**, exhibits one main band at ca 660 nm (15,152 cm^{-1}) due to $^4A_2(F) \rightarrow {}^4T_1(P)(\upsilon_3)$ suggesting tetrahedral geometry [26]. However, the electronic spectra of the other Co(II) complexes **5** and **9** show d–d transitions around 579–568 and 689–677 nm (17,271–17,606 and 14,514–14,771 cm^{-1}) may assignable to $^4T_{1g}(F) \rightarrow {}^4A_{2g}(F)(\upsilon_2)$ and $^4T_{1g}(F) \rightarrow {}^4T_{1g}(P)(\upsilon_3)$ transitions in addition to another band at 465–443 nm (21,505–22,573 cm^{-1}) refers to the charge transfer band suggest an octahedral geometry [46].

All Ni(II) complexes **2**, **6** and **10** were found to be paramagnetic which exclude the possibility of the square planar geometry. Their spectra show three bands at 462–471, 538–529 and 758–748 nm (21,645–21,231, 18,587–18,904 and 13,193–13,369 cm^{-1}) may assignable to $^3A_{2g}(F) \rightarrow {}^3T_{2g}(F)(\upsilon_1)$, $^3A_{2g}(F) \rightarrow {}^3T_{1g}(F)(\upsilon_2)$ and $^3A_{2g}(F) \rightarrow {}^3T_{1g}(P)(\upsilon_3)$ transition suggesting high-spin Ni(II) complex with octahedral configuration, the band at 397–384 nm (25,189–26,042 cm^{-1}) refers to the charge transfer band [47].

The electronic spectra of copper(II) complexes **3** and **11**, display a broad low intensity band centered at 558–549 and 670–661 nm (17,921–18,215 and 14,925–15,129 cm^{-1}) region has been assigned to $^2B_{1g} \rightarrow {}^2A_{1g}$ and $^2B_{1g} \rightarrow {}^2E_g$ transitions suggesting a distorted octahedral environment [48]. Although three transitions are expected in this case due to $^2B_{1g} \rightarrow {}^2A_{1g}(\upsilon_1)$, $^2B_{1g} \rightarrow {}^2B_{2g}(\upsilon_2)$, and $^2B_{1g} \rightarrow {}^2E_g(\upsilon_3)$, transitions, they are very close in energy and often appear in the form of one or two broad bands envelope [49]. The other Cu(II) complex **7** shows a broad and low energy

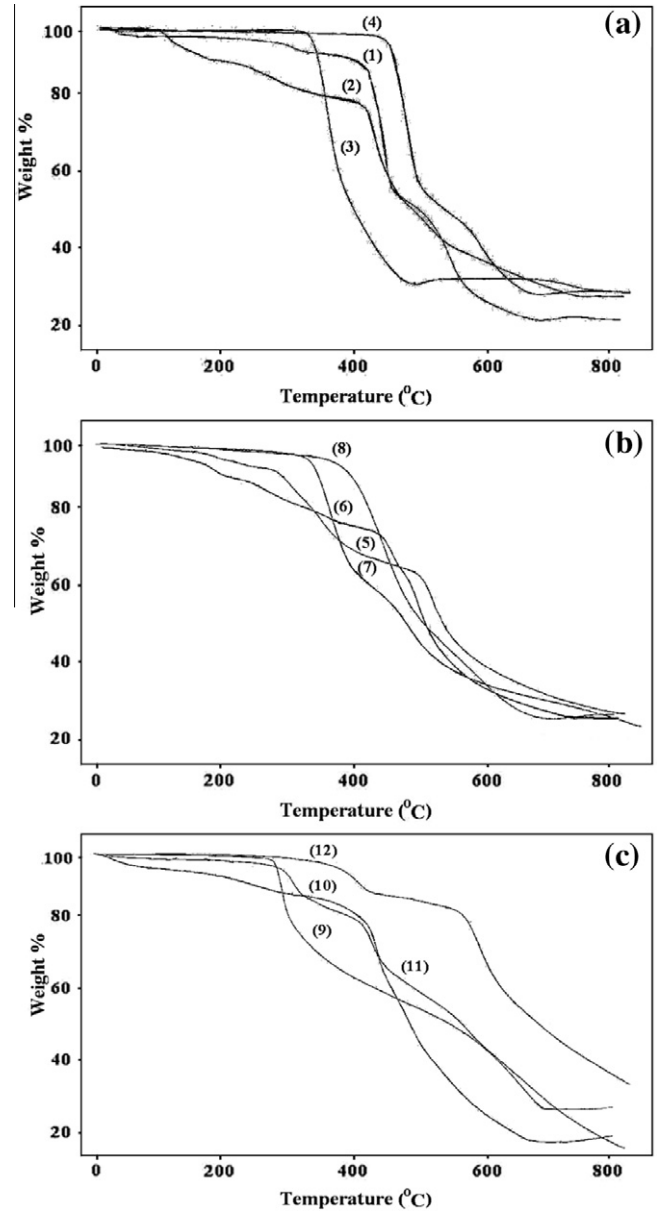

Fig. 8. TGA curves of (a) Binary complexes, (**1**–**4**); (b) Ternary complexes with 2-aminopyridine, (**5**–**8**), (c) Ternary complexes with 8-hydroxyquinoline, (**9**–**12**).

Table 4
Electronic parameters data of octahedral cobalt(II) and nickel(II) complexes*.

Complex[a] No.	Absorption bands (cm^{-1})/peak assignment			Dq (cm^{-1})	B (cm^{-1})	β	β (%)	LFSE (cm^{-1})
	υ_1	υ_2	υ_3					
(5)		14,771	17,606	788	757	0.68	32.41	6300
(9)		14,514	17,271	775	788	0.70	29.64	6198
		$^4T_{1g}(F) \rightarrow {}^4A_{2g}(F)$	$^4T_{1g}(F) \rightarrow {}^4T_{1g}(P)$					
(2)	13,298	18,587	21,645	13,298	527	0.49	51.20	15,958
(6)	13,193	18,904	21,459	13,193	588	0.54	45.56	15,832
(10)	13,369	18,727	21,231	13,369	536	0.50	50.37	16,043
	$^3A_{2g}(F) \rightarrow {}^3T_{2g}(F)$	$^3A_{2g}(F) \rightarrow {}^3T_{1g}(F)$	$^3A_{2g}(F) \rightarrow {}^3T_{1g}(P)$					

The lowering in the (B) values compared to the free metal ion values (1120 and 1080 for Co(II) and Ni(II) ions, respectively) suggests appreciable amount of the covalent character in the metal-ligand bonds. Additionally, (β) value is less than unity suggesting a largely covalent bond between the organic ligands and metal (II) ions in these complexes.
[a] (5 and 9) are cobalt(II) complexes; (2, 6 and 10) are nickel(II) complexes.
* The ligand field splitting energy (Dq), interelectronic repulsion parameter (B), nephelauxetic ratio (β) and ligand field stabilization energy (LFSE).

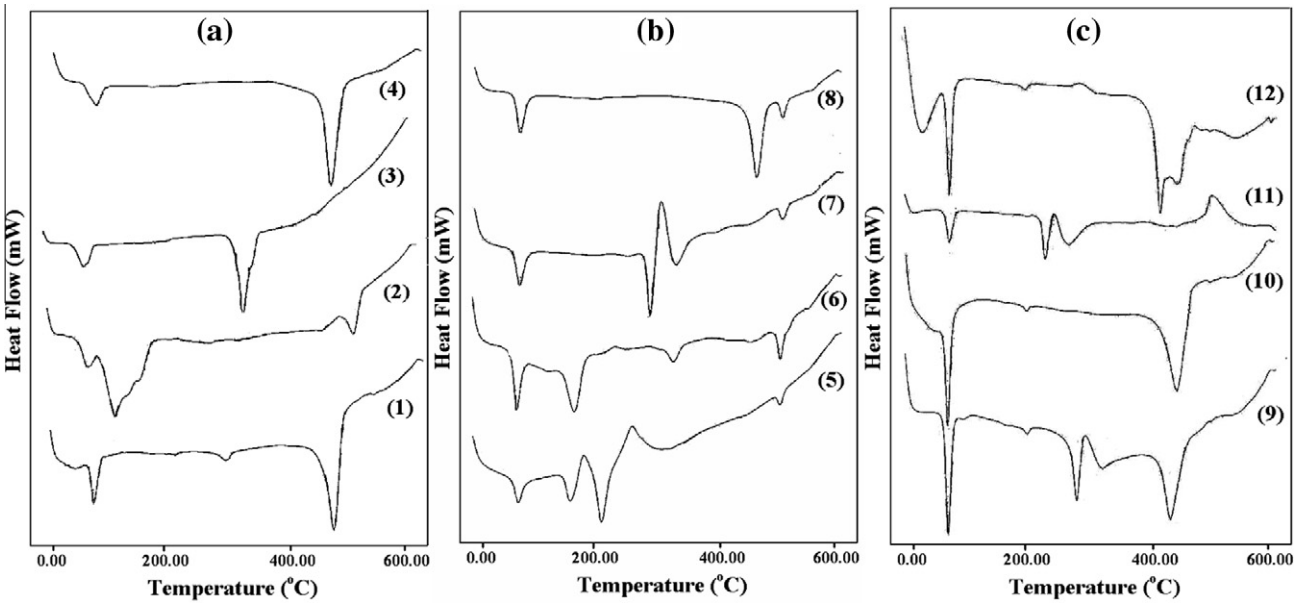

Fig. 9. DSC curves of (a) binary complexes, (**1**–4); (b) ternary complexes with 2-aminopyridine, (**5**–**8**) (c) ternary complexes with 8-hydroxyquinoline, (**9**–**12**).

band at 549 nm (18,215 cm^{-1}) which is attributed to $^2B_{1g} \rightarrow {}^2A_{1g}$ transition which strongly favors the square-planar geometry around the metal ion [50].

Zn(II) complexes **4**, **8** and **12** do not exhibit d–d electronic transition due to completely filled *d*-orbital and show absorptions only in the higher frequency region at 239–222, 367–321 and 451–421 nm (41,841–45,045, 27,248–31,153 and 22,173–24,272 cm^{-1}) attributed to the ligand electron transitions and with the aid of the elemental analysis and other spectroscopic techniques, it is believed that these complexes have a coordination number equal to four as well as six and are likely to be tetrahedral and octahedral structure [18,51].

Various ligand field parameters (D_q, B and β) in addition to LFSE were calculated for the octahedral Co(II) and Ni(II) complexes. The parameters ($10D_q$) and (B) have been calculated from (υ_2) and (υ_3) for Co(II) complexes while in Ni(II) complexes, (υ_1) directly gives the value of ($10D_q$) [26]. A summary of the electronic spectra and ligand field parameters collected are given in Table 4 and agree well with those reported for similar complexes.

Thermal analyses (TG–DSC) of the complexes

The thermal properties of the binary and ternary complexes **(1–12)**, were investigated by thermogravimetric analysis (TGA) and differential scanning calorimetry (DSC), Figs. 8 and 9. The results of the TG–DSC analyses of all complexes as the decomposition stages, temperature ranges, decomposition products, the found and calculated weight loss as well as the probable residue and heat of reaction are given in Table 5. The results show good agreement with the previous suggested formula of the complexes and revealed the following:

- Complexes **1**, **2**, **5**–**7**, **9** and **10** become anhydrous at 102–175 °C. The loss of hydrated water molecules in these complexes was accompanied by an endothermic peak at 77–103 °C with ΔH, 37.50–65.51 J/g.
- The coordinated water molecules were eliminated from the complexes at relatively higher temperatures than the hydrated water [52]. There are two routes in the removal of coordinated water molecules from the complexes which are described below:
  (1) The coordinated water molecules were eliminated in a separate step, as in complexes **2**, **5**, **6**, **8**, **10** and **12**. The elimination of coordinated water molecules in this step (182–340 °C) leads to an isolable complex and was accompanied by an endothermic peak at 141–222 °C with ΔH, 2.38–360.40 J/g.
  (2) Elimination of a coordinated water molecule is accompanied by degradation of the organic part as in complexes **3**, **9** and **11**. In these complexes, elimination of a coordinated water molecule is accompanied by loss of (H_2S and C_6H_5–C_6H_5), (CO_2) and (SO and C_6H_5–C_6H_5), respectively at 345–419°C and was accompanied by an endothermic peak at 206–286 °C with ΔH, 1.66–294.00 J/g. This process leads to a non-isolable complex.
- The TG curve of complex **4**, shows that it is thermally stable up to 277 °C, above which point partial decomposition of the complex begins indicating the absence of water molecules in the complex.
- Comparing the thermal stabilities of anhydrous metal complexes on the basis of initial temperature of decomposition [53], the highest thermal stability is displayed by the complex (**4**) and the sequence of increasing thermal stability was observed as: **4** > **11** > 7 > **8** > **5** > **2** > **3** > **9** > **10** > **1** > **6** > **12**.
- For making evident the influence of 2-Ampy and 8-OHqu as a secondary ligands on the thermal stability of the metal complexes, we have determined T_i (initial temperature) and T_f (final temperature) corresponding the first TGA peak for anhydrous complexes. The results are presented in Table 6. From these data examination one can observe the influence of the ligands structure on these parameters as clear in Fig. 10.

Powder X-ray diffraction characterization

The powder X-ray diffraction patterns of the ligand and its binary and ternary complexes, (**1**–**12**) have been recorded in a scanning range of 5–80° (2θ) and depicted in Fig. 11. Table 7 shows the observed diffraction data, i.e., inter planar spacing d (Å), relative intensities (I/I_0) and (2θ) observed of the ligand and its binary and ternary nickel(II) complexes, (**2**, **6** and **10**) as representative example. From the patterns plotted in Fig. 11, we can observe that the diffraction peaks of all metal complexes, in terms of location, numbers or intensity are different from the ligand, indicating that

Table 5
Thermal analyses data (TG–DSC) for binary and ternary complexes.

Compd. no.	Emperical formula	Temp. range (°C)	% Weight loss found (Calcd.)	Lost fragment (no. of molecules)	Probable residue found/ (Calcd.)	DSC peak (°C)		
						Endo	Exo	ΔH (J/g)
(**1**)	$[Co(HL)Cl]\cdot½H_2O$	45–106	2.24(2.29)	$½H_2O$ (hyd.)	$CoC_{14}H_{12}NO_4SCl$	100	–	56.78
	$CoC_{14}H_{12}NO_4SCl.0\cdot5H_2O$	108–350	4.99(4.06)	$½O_2$	$CoC_{14}H_{12}NO_3SCl$	222	–	3.02
		351–475	37.83(38.41)	CH_3CN and C_6H_5SH	$CoC_6H_3O_3Cl$	301	–	13.01
		475–595	29.30(29.09)	CO, HCl and HC≡C–C≡CH	$CoCO_2$	468	–	314.16
		595–699	6.69(7.11)	CO	CoO; 18.95(19.03)	526	–	31.4
(**2**)	$[Ni(HL)Cl(H_2O)_2]\cdot1½H_2O$	38–165	6.00(6.04)	$1½H_2O$ (hyd.)	$NiC_{14}H_{12}NO_4SCl\cdot2H_2O$	99	–	37.5
	$NiC_{14}H_{12}NO_4SCl.3\cdot5H_2O$	165–270	7.23(8.05)	$2H_2O$ (coord.)	$NiC_{14}H_{12}NO_4SCl$	141	–	360.4
		271–413	9.81(9.83)	CO_2	$NiC_{13}H_{12}NO_2SCl$	283	–	6.02
		415–490	31.20(31.33)	NO and C_6H_5SH	NiC_7H_6OCl	327	–	3.87
		490–562	13.75(13.74)	$½Cl_2$ and HC≡CH	NiC_5H_4O	454	–	4.83
		563–772	15.01(14.30)	All remaining ligand	NiO; 17.00(16.96)	505	–	66.37
(**3**)	$[Cu(HL)(H_2O)_3]Cl$	125–393	55.12(54.66)	$3H_2O$(coord.), H_2S and C_6H_5—C_6H_5	CuC_2NO_4Cl	206	–	1.66
	$CuC_{14}H_{12}NO_4SCl\cdot3H_2O$	393–482	24.38(24.24)	CO, CO_2 and $½Cl_2$	CuNO	341	–	190.84
		483–790	3.18(3.16)	$½N_2$	CuO; 17.32(17.90)	452	–	2.41
(**4**)	[Zn(HL)Cl]	277–507	50.13(50.17)	$½O_2$, CN and C_6H_5—C_6H_5	$ZnCH_2O_3SCl$	103	–	49.81
	$ZnC_{14}H_{12}NO_4SCl$	508–559	8.72(9.06)	$½Cl_2$	$ZnCH_2O_3S$	461	–	259.08
		560–778	20.69(19.97)	CO_2 and H_2S	ZnO; 20.46(20.81)	523	–	8.2
(**5**)	[Co(HL)(2-Ampy)Cl(H_2O)]·$½H_2O$	39–167	2.41(1.78)	$½H_2O$ (hyd.)	$CoC_{19}H_{18}N_3O_4SCl\cdot H_2O$	103	–	62.87
	$CoC_{19}H_{18}N_3O_4SCl.1\cdot5H_2O$	168–231	2.93(3.56)	H_2O (coord.)	$CoC_{19}H_{18}N_3O_4SCl$	182	–	106.22
		232–281	2.16(2.77)	$½N_2$	$CoC_{19}H_{18}N_2O_4SCl$	323	–	298.67
		283–339	9.80(10.29)	2CN	$CoC_{17}H_{18}O_4SCl$	442	–	3.56
		339–496	21.73(20.99)	CH_2=CH_2 and C_6H_6	$CoC_9H_8O_4SCl$	505	–	17.84
		497–790	43.16(42.62)	O_2, CO_2, Cl, HC≡CH and C_6H_6	CoS; 17.81(17.99)	532	–	11.26
(**6**)	[Ni(HL)(2-Ampy)Cl(H_2O)]·$½H_2O$	34–102	1.17(1.78)	$½H_2O$ (hyd.)	$NiC_{19}H_{18}N_3O_4SCl\cdot H_2O$	77	–	61.91
	Ni $C_{19}H_{18}N_3O_4SCl.1\cdot5H_2O$	103–182	3.76(3.56)	H_2O (coord.)	$NiC_{19}H_{18}N_3O_4SCl$	190	–	85.51
		184–224	4.47(5.15)	CN	$NiC_{18}H_{18}N_2O_4SCl$	–	252	−9.3
		224–332	9.86(9.51)	SO	$NiC_{18}H_{18}N_2O_3Cl$	341	–	18.81
		334–425	7.08(7.01)	$½Cl_2$	$NiC_{18}H_{18}N_2O_3$	459	–	4.91
		426–477	14.34(14.25)	CN and NO_2	$NiC_{17}H_{18}O$	505	–	22.41
		478–791	47.14(48.06)	CO, $2CH_2$=CH_2 and C_6H_5—C_6H_5	Ni; 11.26(11.60)	543	–	4.45
(**7**)	[Cu(HL)(2-Ampy)]Cl.$½H_2O$	35–175	2.48(1.83)	$½H_2O$ (hyd.)	$CuC_{19}H_{18}N_3O_4SCl$	103	–	62.01
	$CuC_{19}H_{18}N_3O_4SCl.0\cdot5H_2O$	175–403	26.90(27.44)	O_2 and C_6H_5CN	$CuC_{12}H_{13}N_2O_2SCl$	320	–	238.59
		404–537	19.09(19.31)	$½O_2$ and C_5H_5N	CuC_7H_8NOSCl	436	–	17.44
		537–798	11.04(10.65)	$½O_2$ and HCl	CuS and Organic part; 40.49(40.77)	542	–	7.67
(**8**)	[Zn(HL)(2-Ampy)Cl(H_2O)]	175–336	2.90.(3.58)	H_2O (coord.)	$ZnC_{19}H_{18}N_3O_4SCl$	221	–	4.09
	$ZnC_{19}H_{18}N_3O_4SCl\cdot H_2O$	339–527	53.62(53.60)	HCl, C_5H_5N and C_6H_5—C_6H_5	$ZnC_2H_2N_2O_4S$	466	–	150.02
		527–700	24.36(23.46)	$2NO_2$ and HC≡CH	ZnS; 19.12(19.36)	543	–	3.8
(**9**)	[Co(HL)(8-Oqu)(H_2O)]·$½H_2O$	43–119	1.39(1.73)	$½H_2O$ (hyd.)	$CoC_{23}H_{18}N_2O_5S\cdot H_2O$	102	–	65.51
	$CoC_{23}H_{18}N_2O_5S.1\cdot5H_2O$	121–345	11.89(11.92)	H_2O (coord.) and CO_2	$CoC_{22}H_{18}N_2O_3S$	221	–	294
		345–423	7.96(7.69)	$½N_2$ and CN	$CoC_{21}H_{18}O_3S$	297	–	42.26
		423–466	14.03(14.24)	SO and HC≡CH	$CoC_{19}H_{16}O_2$	336	–	39.63
		466–603	23.04(23.09)	HC≡CH and C_6H_5OH	$CoC_{11}H_8O$	441	–	83.74
		603–789	27.88(26.94)	All remaining ligand	CoO; 13.81(14.39)	519		31.43
(**10**)	[Ni(HL)(8-Oqu)(H_2O)]·$1½H_2O$	39–110	4.12(5.02)	$1½H_2O$ (hyd.)	$NiC_{23}H_{18}N_2O_5S\cdot H_2O$	103	–	59.9
	$NiC_{23}H_{18}N_2O_5S.2\cdot5H_2O$	111–208	2.43(3.35)	H_2O (coord.)	$NiC_{23}H_{18}N_2O_5S$	222	–	2.65
		209–317	5.69(5.21)	N_2	$NiC_{23}H_{18}O_5S$	361	–	3.47
		319–460	27.67(27.52)	O_2, SO_2 and 2HC≡CH	$NiC_{19}H_{14}O$	452	–	165.56
		460–535	25.16(24.94)	$2CH_2$=CH_2 and C_6H_6	NiC_9O	502	–	901
		535–702	20.74(20.08)	9C	NiO; 14.19(13.88)	529	–	26.39
(**11**)	[Cu(HL)(8-Oqu)(H_2O)]	275–419	42.95(42.69)	H_2O (coord.), SO and C_6H_5—C_6H_5	$CuC_{11}H_8N_2O_4$	286	–	140.41
	$CuC_{23}H_{18}N_2O_5S\cdot H_2O$	419–577	18.58(18.24)	C_6H_5OH	$CuC_5H_2N_2O_3$	449	–	25.56
		578–680	26.26(26.76)	2HCN and 3CO	Cu; 12.21(12.31)	–	501	−167.3
(**12**)	[Zn(HL)(8-Oqu)(H_2O)]	38–340	3.28(3.48)	H_2O (coord.)	$ZnC_{23}H_{18}N_2O_5S$	222	–	2.38
	$ZnC_{23}H_{18}N_2O_5S\cdot H_2O$	341–434	9.88(10.05)	2HC≡CH	$ZnC_{19}H_{14}N_2O_5S$	–	304	7.65
		436–536	4.44(5.02)	HC≡CH	$ZnC_{17}H_{12}N_2O_5S$	427	–	25.67
		537–631	27.85(27.84)	HC≡C—C≡CH and C_6H_5OH	$ZnC_7H_4N_2O_4S$	452	–	19.55
		631–794	23.30(22.42)	$½N_2$,CN,HC≡C—C≡CH and HC≡CH	$ZnSO_4$; 31.25(31.19)	542	–	39.17

Table 6
The initial and final decomposition temperatures (°C) of binary complexes in comparison to ternary complexes.

Metal complexes			
	(1) [Co(HL)Cl]·½H_2O	**(5)** [Co(HL)(2-Ampy)Cl(H_2O)]·½H_2O	**(9)** [Co(HL)(8-Oqu)(H_2O)]·½H_2O
T_i	108	168	121
T_f	350	231	345
	(2) [Ni(HL)Cl(H_2O)$_2$]·1½H_2O	**(6)** [Ni(HL)(2-Ampy)Cl(H_2O)]·½H_2O	**(10)** [Ni(HL)(8-Oqu)(H_2O)]·1½H_2O
T_i	165	103	111
T_f	270	182	208
	(3) [Cu(HL)(H_2O)$_3$]Cl	**(7)** [Cu(HL)(2-Ampy)]Cl.½H_2O	**(11)** [Cu(HL)(8-Oqu)(H_2O)]
T_i	125	175	275
T_f	393	403	419
	(4) [Zn(HL)Cl]	**(8)** [Zn(HL)(2-Ampy)Cl(H_2O)]	**(12)** [Zn(HL)(8-Oqu)(H_2O)]
T_i	277	175	38
T_f	507	336	340

T_i is the initial decomposition temperature.
T_f is the final decomposition temperature.

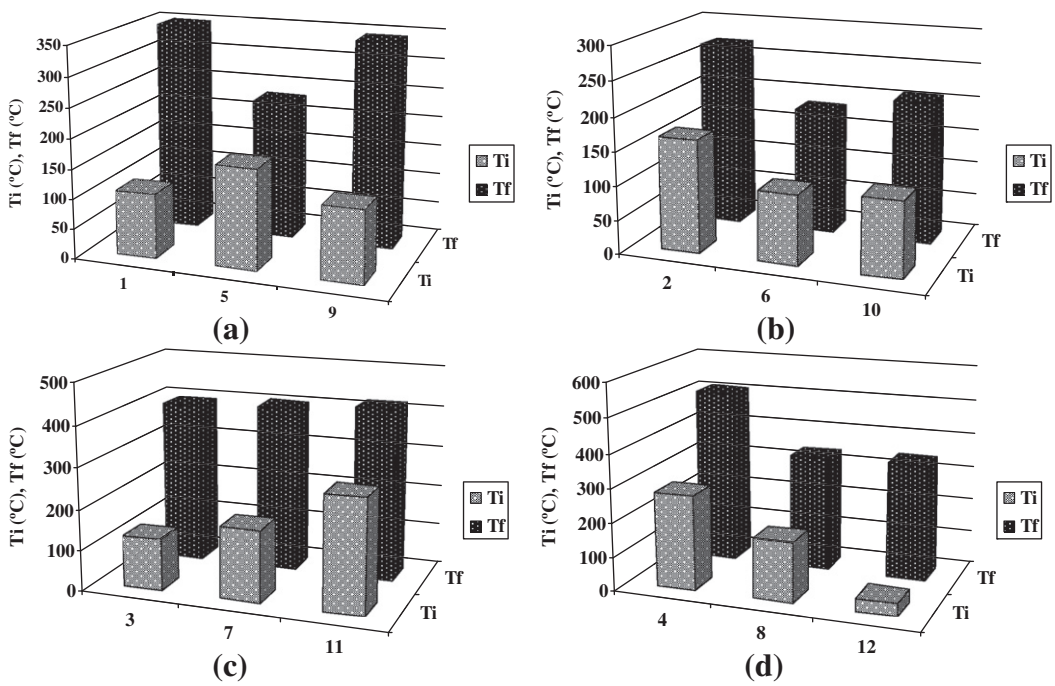

Fig. 10. The initial (T_i) and final (T_f) decomposition temperatures of binary complexes in comparison to ternary complexes: (a) binary and ternary Co(II) complexes, (b) binary and ternary Ni(II) complexes, (c) binary and ternary Cu(II) complexes and (d) binary and ternary Zn(II) complexes.

the reaction produced a new crystalline phase, that is, the complex has been formed [54]. All metal complexes show crystalline phase with different degree of crystalinity except the complexes **1**, **3**, **4** and **8** which have poor diffractions. With the help of the data obtained from the powder XRD, the crystallite size calculations were performed using Scherrer equation [55,56] and the values obtained for crystallite size, Table 8 indicated that the particles were of nano-sized.

Qualitative and quantitative antimicrobial assay results

In testing the antibacterial and antifungal activity of the newly synthesised compounds, we used more than one test organism to increase the chance of detecting antibiotic principles in tested materials. Qualitative and quantitative results for antimicrobial assays are given in Table 9 in addition to the calculated percent activity index data [57]. Figs. 12 and 13 are graphical representation of antibacterial and antifungal data of all compounds under study. Analyzing the tabulated antimicrobial screening results allows us to conclude that:

- The ligand as well as its complexes shows a significant degree of antimicrobial activity against the organisms and the activity increases as the concentration of the synthesised compounds increases [58].
- The remarkable result is that: (a) the synthesised compounds showed lower inhibition against *A. fumigates* as compared with the other organisms. They display low activity (mean of zone diameter is 5–12 mm $\leqslant$ 1/3 of mean zone diameter of reference standard, 12.3 mm); (b) The ligand does not have any activity against *E. coli*, additionally, some complexes showed no activity towards the different organisms. This may be attributed to the less lipophilic character which does not favor their permeation through the lipoid layer of microbial membranes [59].
- Generally, the ligand and its metal complexes show varying degrees of antimicrobial activity and the metal complexes show better activity than the ligand. Some principal factors should be considered for such activity: (i) the chelate effect, (ii) the nature of the ligand; (iii) the total charge of the complex; (iv) the nature of the ion neutralizing the ionic complex;

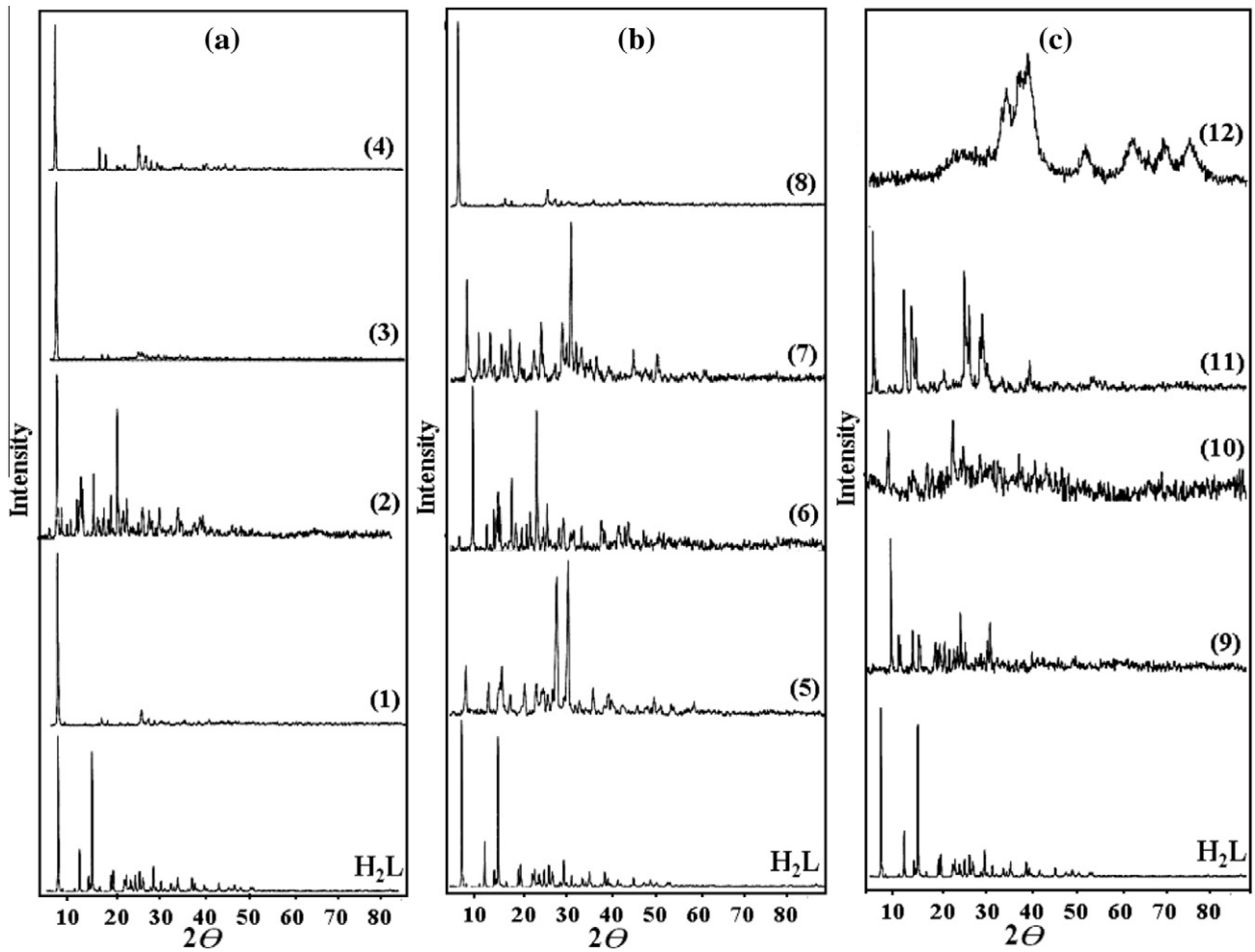

Fig. 11. X-ray powder diffraction patterns of: (a) Schiff base ligand, H_2L and its binary complexes, (**1**–**4**), (b) Schiff base ligand, H_2L and its ternary complexes with 2-aminopyridine, (**5**–**8**), (d) Schiff base ligand, H_2L and its ternary complexes with 8-hydroxyquinoline, (**9**–**12**).

(v) the nuclearity of the metal center in the complex [60]. Thus, in our study, the enhancement in the activity upon complexation can be explained on the basis of chelation theory. Such a chelation could enhance the lipophilic character of the central metal atom, which subsequently favors it permeation through the lipid layers of cell membrane and blocking the metal binding sites on enzymes of microorganism. The variation in the effectiveness of different compound against different organisms also depends on a nature of the metal ion, nature of the ligand, geometry of the complex, and impermeability of the cell of the microbes or differences in ribosomes of microbial cells. It is also suspected that factors such as solubility, conductivity, dipole moment (influenced by the presence of metal ions) may be the possible reasons for the increase in activity [61].

- On comparison of all metal complexes, the binary Co(II) complex, (**1**) has the highest inhibition against *S. aureus* and *C. albicans*, it exhibits higher activity (mean of zone diameter, 25 and 27 mm, respectively is >2/3 of mean zone diameter of reference standard, 23.3 mm), moreover, the ternary Cu(II) complex (**7**) has the highest inhibition against *C. albicans*, (mean of zone diameter is 26 mm). All other complexes showed either low activity, intermediate activity or inactive against the various strains.
- The quantitative antimicrobial results via minimum inhibitory concentration studies, Table 10, showed that:

(i) All metal complexes under study inhibit the growth of *C. albicans* more than the other organisms with a MIC range of 4–8 μg/mL. Also, the complexes**1**–**4** and **7**–**11** have the same effect towards *B. subtilis*.

(ii) The ternary Zn(II) complex, (**12**) was very effective against *B. subtilis* than all other complexes with a MIC value of 2 μg/mL.

(iii) The complexes **1**, **2** and **7**–**11** have a smaller effectiveness (MIC 128 μg/mL) towards *E. coli*.

Structural interpretation

The reaction of the Schiff base ligand, H_2L with the metal ions Co(II), Ni(II), Cu(II) or Zn(II) yielded binary mononuclear complexes, **1**–**4**. Also, the ternary complexes were prepared using 2-aminopyridine or 8-hydroxyquinoline as secondary ligands to give the complexes, **5**–**8** and **9**–**12**, respectively. Correlation of all spectroscopic data suggest that the Schiff base ligand H_2L act as monoanionic terdentate ligand with ONO sites coordinating to the metal ions via deprotonated phenolic-O, azomethine-N and sulfonate-O. The secondary ligand, 2-aminopyridine behaves as a neutral monodentate ligand via the amino group-N while 8-hydroxyquinoline behaves as a monoanionic bidentate ligand through the ring-N and deprotonated phenolic-O. The metal complexes have tetrahedral, square planar or octahedral configurations and the structure is shown in Figs. 2–4.

Table 7
X-ray diffraction data of ligand, (H_2L) and its nickel(II) complexes.[a]

Peak no.	H_2L			(2) $[Ni(HL)Cl(H_2O)_2]\cdot 1½H_2O$			(6) $[Ni(HL)(2\text{-Ampy})Cl(H_2O)]\cdot ½H_2O$			(10) $[Ni(HL)(8\text{-Oqu})(H_2O)]\cdot 1½H_2O$		
	d (Å)	Intensity (%)	2θ	*d* (Å)	Intensity (%)	2θ	*d* (Å)	Intensity (%)	2θ	*d* (Å)	Intensity (%)	2θ
1	12.32	100.00	7.17	13.23	6.90	6.68	15.49	8.90	5.70	10.55	86.10	8.37
2	7.54	27.3	11.72	10.53	100.00	8.39	10.45	100.0	8.45	7.10	29.80	12.46
3	6.50	10.60	13.61	9.52	19.90	9.28	7.88	16.00	11.22	5.52	45.30	16.05
4	6.14	90.40	14.42	8.44	9.40	10.48	7.00	25.30	12.63	5.20	38.20	17.05
5	4.81	10.60	18.42	7.87	12.80	11.23	6.57	35.70	13.46	4.20	100.00	21.13
6	4.69	13.90	18.91	7.03	24.90	12.58	6.38	26.70	13.87	3.84	64.60	23.13
7	4.17	7.90	21.31	6.60	36.70	13.40	5.46	44.60	16.21	3.37	54.90	26.47
8	4.09	10.50	21.71	6.42	31.70	13.79	5.20	16.50	17.04	2.62	56.20	34.16
9	3.93	7.80	22.59	5.47	41.60	16.18	4.86	14.30	18.23	2.12	41.50	42.57
10	3.76	10.50	23.63	5.19	11.80	17.07	4.62	16.50	19.22	2.10	28.60	43.11
11	3.62	13.50	24.56	4.84	16.30	18.33	4.46	23.30	19.88	2.06	24.90	43.89
12	3.53	9.00	25.24	4.59	12.30	19.31	4.17	84.60	21.28	1.76	22.40	51.78
13	3.24	15.70	27.53	4.47	27.90	19.86	3.93	14.40	22.58	1.73	17.70	52.82
14	3.06	6.80	29.15	4.18	83.50	21.25	3.81	28.50	23.31	1.49	34.50	62.27
15	2.74	9.10	32.68	3.95	17.00	22.51	3.47	13.70	25.63	1.41	16.50	66.08
16	2.51	9.00	35.76	3.83	25.60	23.24	3.35	19.80	26.57	1.23	37.20	77.62
17				3.47	9.40	25.65	3.19	10.20	27.98	1.22	36.20	78.25
18				3.35	19.90	26.60	3.11	12.70	28.64			
19				3.18	18.30	28.04	2.95	14.80	30.22			
20				3.12	10.80	28.61	2.62	18.10	34.17			
21				3.03	6.90	29.44	2.57	12.10	34.87			
22				2.95	19.80	30.23	2.39	12.90	37.61			
23				2.74	7.20	32.63	2.32	14.20	38.87			
24				2.62	19.60	34.16	2.28	15.00	39.53			
25				2.57	11.30	34.84	2.12	12.40	42.62			
26				2.38	10.30	37.78	1.94	11.20	46.70			
27				2.31	12.60	38.97	1.90	8.00	47.71			
28				2.28	14.10	39.52	1.71	6.40	53.46			
29				2.17	6.00	41.61	1.40	6.10	66.63			
30				1.98	8.20	45.79	1.35	6.80	69.52			
31				1.89	6.00	48.14	1.31	6.60	72.23			
32				1.82	6.40	50.13						

[a] Intensity (%) less than 6% was omitted.

Table 8
Particle sizes of the ligand, H_2L and its metal complexes.

Comp. no.[a]	2θ	*d* (Å)	FWHM	Cryst. size[b]
H_2L	7.17	12.32	1.200×10^{-3}	129.80
(**2**)	8.39	10.53	2.816×10^{-3}	55.30
(**5**)	27.68	3.22	4.584×10^{-3}	34.30
(**6**)	8.45	10.45	2.030×10^{-3}	76.70
(**7**)	25.26	3.52	3.383×10^{-3}	46.20
(**9**)	9.28	9.53	2.139×10^{-3}	72.80
(**10**)	21.13	4.20	5.369×10^{-3}	28.90
(**11**)	5.75	15.37	2.357×10^{-3}	66.40
(**12**)	35.72	2.51	8.512×10^{-3}	3.00

[a] Crystallite size of complexes **1**, **3**, **4** and **8** cannot be calculated.
[b] Crystallite size obtained using Scherrer's equation, $D = K\lambda/(\beta\cos\theta)$ where D is the particle size in nm of the crystal gain has been calculated using maximum intensity peak; K is Scherrer's constant; λ is the wavelength of target used; β is the full width at half maximum reflection height in terms of radian and θ is Bragg diffraction angle at peak position in degree.

Experimental

Analysis and physical measurements

All chemicals used were of highest available purity, were BDH, Analar, Sigma, or Merck products. They are: cobalt chloride hexahydrates, nickel chloride hexahydrates, copper chloride dihydrates and zink chloride unhydrous, salicylaldehyde, 2-aminopyridine, 8-hydroxyquinoline, 4-Aminotoluene-3-sulfonic acid, absolute ethyl alcohol, diethylether, dimethylformamide and dimethylsulfoxide. Concentrated nitric acid was reagent grade and used as supplied.

Microanalyses of carbon, hydrogen, nitrogen and sulfur contents were determined using a Perkin–Elmer 2408 CHN analyzer. Metal contents were determined complexometry after complete decomposition of their complexes with concentrated nitric acid in a Kjeldal flask, while the chlorine content was determined gravimetrically as AgCl [62]. Melting or decomposition points were carried out on a melting point apparatus, Gallenkamp, England. Molar conductance measurements were measured in solutions of the metal complexes in DMF (10^{-3} M) using WTWD-812 Weilheium-Conductivity meter model LBR, fitted with a cell model LTA100. IR spectra were recorded on a Perkin–Elmer FT-IR type 1650 spectrophotometer using KBr discs. ^{1}H NMR spectra were recorded using Brucker ARX-300 spectrometer using DMSO-d_6 as a solvent, chemical shifts are reported in parts per million. Mass spectra were recorded in a range of m/e ratio between 0 and 1000 on a Jeol JMSAX-500 mass spectrometer. The solid reflectance spectra of the ligand and its metal complexes were recorded on a Jasco model V-550 UV–Vis spectrophotometer. Magnetic susceptibility of the metal complexes was measured by the Gouy method at room temperature using a Johnson Matthey, Alpha products, model MKI magnetic susceptibility balance. TG–DSC measurements were carried out on a Shimadzu thermogravimetric analyzer using the TA-50 WSI program. X-ray powder diffraction analysis were carried out at ambient temperature with a Shimadzu 160D X-ray diffractometer using Cu Kα radiation over the range ($4 < 2\theta < 80$), with steps of 0.01° and a step time of 2 s. The antimicrobial activity of the ligand and its complexes were screened using the standardized disk-agar diffusion method [18], moreover, the agar dilution technique was used in minimum inhibitory concentration (MIC) study [20].

Table 9
Antimicrobial screening results of all compounds under study.

Sample	Organism											
	Gram-positive bacteria				Gram-negative bacteria				Yeasts		Fungi	
	Staphylococcus aureus (ATCC 25923)		*Bacillus subtilis* (ATCC 6635)		*Salmonella typhimurium* (ATCC 14028)		*Escherichia coli*		*Candida albicans* (ATCC 25922)		*Aspergillus fumigatus* (ATCC 10231)	
	Conc.											
	1 mg/mL	0.5 mg/mL	1 mg/mL	0.5 mg/mL	1 mg/mL	0.5 mg/mL	1 mg/mL	0.5 mg/mL	1 mg/mL	0.5 mg/mL	1 mg/mL	0.5 mg/mL
H_2L	8(23)	6(23)	5(14)	3(12)	9(25)	6(21)	–	–	6(17)	5((18)	5(14)	4(15)
(1)	25(71)	15(58)	20(57)	18(72)	21(58)	18(64)	19(50)	17(63)	27(77)	24(86)	–	–
(2)	18(51)	10(38)	15(43)	13(50)	15(42)	14(50)	16(42)	13(48)	16(46)	14(50)	8(22)	7(27)
(3)	–	–	18(51)	14(56)	15(42)	12(43)	–	–	22(63)	18(64)	–	–
(4)	–	–	18(51)	15(60)	–	–	15(38)	10(37)	17(49)	14(50)	–	–
(5)	–	–	–	–	8(22)	7(25)	6(16)	2(7)	4(11)	3(11)	6(16)	5(19)
(6)	10(29)	6(23)	11(31)	9(36)	11(31)	9(32)	11(29)	7(25)	19(54)	10(36)	5(14)	3(12)
(7)	17(49)	9(35)	13(37)	10(40)	20(56)	15(54)	11(29)	10(37)	26(74)	18(64)	12(32)	5(19)
(8)	–	–	15(43)	12(48)	20(56)	18(64)	11(29)	8(30)	20(57)	16(57)	–	–
(9)	19(54)	15(58)	14(40)	10(40)	16(44)	15(54)	14(37)	11(41)	22(63)	20(71)	8(22)	7(27)
(10)	20(57)	16(62)	15(43)	12(48)	16(44)	13(46)	14(37)	13(48)	15(43)	14(50)	–	–
(11)	10(29)	7(27)	14(40)	9(36)	18(50)	16(57)	17(45)	8(30)	22(63)	20(71)	12(32)	9(35)
(12)	–	–	20(57)	18(72)	17(47)	15(54)	13(34)	6(22)	23(66)	19(68)	–	–
R.S	35	26	35	25	36	28	38	27	35	28	37	26

• The test was done using the agar–disc diffusion method.
• R.S; Reference standard: *Chloramphencol* and *Cephalothin* were used as standard references for Gram positive bacteria and Gram negative bacteria, respectively and *Cycloheximide* was used as standard reference in case of yeasts and fungi.
• Inhibition values: (a) low activity = mean of zone diameter is ⩽1/3 of mean zone diameter of control, (b) intermediate activity = mean of zone diameter ⩽2/3 of mean zone diameter of control, (c) high activity = mean of zone diameter >2/3 of mean zone diameter of control and (e) no effect.

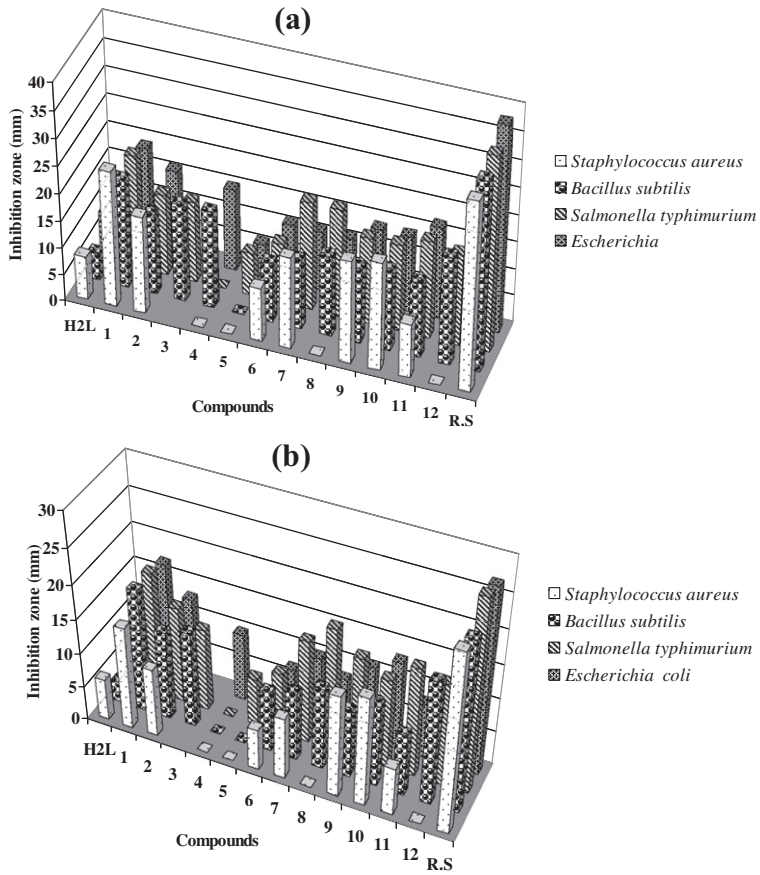

Fig. 12. Antibacterial activity of Schiff base H_2L, ligand and its complexes, (**1**–**12**) at (a) higher concentration and (b) lower concentration.

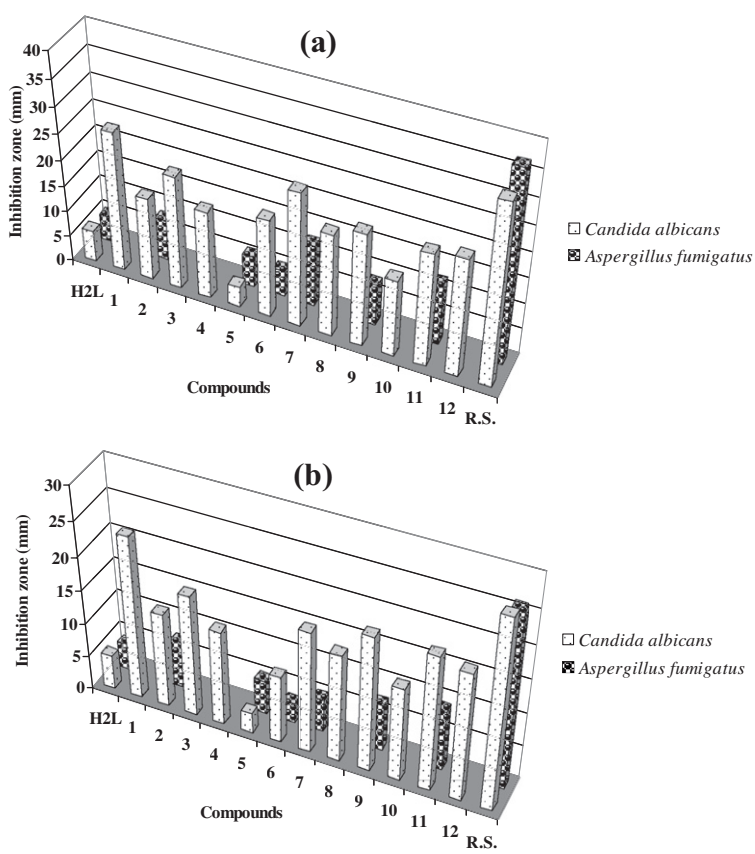

Fig. 13. Antifungal activity of Schiff base H_2L, ligand and its complexes, (**1**–**12**) at (a) higher concentration and (b) lower concentration.

Table 10
Minimum inhibitory concentration (MIC) of synthesised compounds under study.

Sample	MIC μg/mL Organism					
	Gram-positive bacteria		Gram-negative bacteria		Yeasts	Fungi
	Staphylococcus aureus (ATCC 25923)	*Bacillus subtilis* (ATCC 6635)	*Salmonella typhimurium* (ATCC 14028)	*Escherichia coli* (ATCC 25922)	*Candida albicans* (ATCC 10231)	*Aspergillus fumigatus*
(1)	16	8	16	128	8	ND
(2)	32	4	64	128	8	ND
(3)	ND	8	64	ND	4	ND
(4)	ND	4	ND	64	8	ND
(6)	ND	ND	ND	ND	8	ND
(7)	8	4	4	128	4	ND
(8)	ND	4	4	128	8	ND
(9)	8	4	64	128	8	ND
(10)	32	4	16	128	8	ND
(11)	ND	4	16	128	4	ND
(12)	ND	2	16	ND	4	ND
R.S	9	1	13	41	3	2

ND: Not detected under the experimental condition.

Synthesis of Schiff base ligand, H_2L

To an ethanolic solution of 4-aminotoluene-3-sulfonic acid (9.36 g, 0.05 mol), an equimolar quantity of salicylaldehyde (5.31 ml, 0.05 mol) was added drop wise then the reaction mixture were heated to reflux for 5 h. The yellow product obtained was filtered off and washed several times with a few amount of ethyl alcohol then diethyl ether and dried in vacuum desiccators over anhydrous $CaCl_2$. Fig. 1 shows the pathway of ligand preparation.

Synthesis of the Schiff base metal complexes

Preparation of the binary complexes

The metal salt, namely $CoCl_2{\cdot}6H_2O$, $NiCl_2{\cdot}6H_2O$, $CuCl_2{\cdot}2H_2O$ and $ZnCl_2$ anhydrous dissolved in a least amount of distilled water (0.005 mol), was added to a mixture of (0.005 mol) $LiOH{\cdot}H_2O$ and (0.005 mol) H_2L in 40 ml ethanol. After complete addition, the reaction mixture was refluxed for 3 h with constant stirring to ensure the complete formation of metal complexes. The precipitated solid complexes were filtered, washed several times with 50% (v/v) ethanol–water followed by ethyl alcohol then diethyl ether and dried in vacuum desiccators over anhydrous $CaCl_2$.

Preparation of ternary complexes based on 2-aminopyridine

The metal salt, namely $CoCl_2{\cdot}6H_2O$, $NiCl_2{\cdot}6H_2O$, $CuCl_2{\cdot}2H_2O$ and $ZnCl_2$ anhydrous dissolved in a least amount of distilled water (0.005 mol), was added to a mixture of (0.005 mol) $LiOH{\cdot}H_2O$, (0.005 mol) H_2L and (0.005 mol) of 2-Ampy as a secondary ligand in 60 ml ethanol. After complete addition, the reaction mixture was refluxed for 4 h with constant stirring to ensure the complete formation of metal complexes. The precipitated solid complexes were filtered, washed several times with 50% (v/v) ethanol–water followed by ethyl alcohol then diethyl ether and dried in vacuum desiccators over anhydrous $CaCl_2$.

Preparation of ternary complexes based on 8-hydroxyquinoline

The metal salt, namely $CoCl_2{\cdot}6H_2O$, $NiCl_2{\cdot}6H_2O$, $CuCl_2{\cdot}2H_2O$ and $ZnCl_2$ anhydrous dissolved in a least amount of distilled water (0.005 mol), was added to a mixture of (0.005 mol) $LiOH{\cdot}H_2O$, (0.005 mol) H_2L and (0.005 mol) of 8-OHqu as a secondary ligand in 60 ml ethanol. After complete addition, the reaction mixture was refluxed for 4 h with constant stirring to ensure the complete formation of metal complexes. The precipitated solid complexes were filtered, washed several times with 50% (v/v) ethanol–water followed by ethyl alcohol then diethyl ether and dried in vacuum desiccators over anhydrous $CaCl_2$.

Antimicrobial screening

Qualitative antimicrobial assay

Antibacterial and antifungal activity was qualitatively determined using the standardized disk-agar diffusion method [18] described below:

The tested compounds were dissolved in DMF, which has no inhibition activity to get concentrations of 0.5 and 1 mg/mL in DMF. The test was performed on medium potato dextrose agar (PDA), which contains an infusion of 200 g potatoes, 6 g dextrose, and 15 g agar. Uniform size filter paper disks (3 disks per compound) were impregnated by an equal volume (10 μL) from the specific concentration of dissolved tested compounds and carefully placed on inoculated agar surface. After incubation for 36 h at 27 °C in the case of bacteria and for 48 h at 24 °C in the case of fungi, the inhibition zone diameter produced by these compounds against the particular test organism determined the antimicrobial activity of the compound. The mean value obtained for three individual replicates was used to calculate the zone of growth inhibition of each sample. The activity of tested compounds was categorized as (a) low activity = mean of zone diameter is $\leqslant 1/3$ of mean zone diameter of control, (b) intermediate activity = mean of zone diameter $\leqslant 2/3$ of mean zone diameter of control and (c) high activity = mean of zone diameter >2/3 of mean zone diameter of control.

Quantitative antimicrobial assay

The minimum inhibitory concentration (MIC) was evaluated by the macro dilution test using standard inoculums of 10^{-5} - CFU mL^{-1}. Serial dilutions of the test compounds, previously dissolved in dimethylformamide (DMF) were prepared to final concentrations of 256, 128, 64, 32, 16, 8, 4, 2, and 1 μg/ml to each tube was added 100 μL of a 24 h old inoculum. The MIC was determined visually after incubation for 24 h, at 37 °C [20].

References

[1] L. Pejov, M. Ristova, B. Soptrajanov, Spectrochim. Acta Part A 79 (2011) 27.
[2] S. Riediker, M.J.F. Suter, W. Giger, Wat. Res. 34 (2000) 2069.
[3] E. Ayranci, O. Duman, Chem. Eng. J. 156 (2010) 70.
[4] K. Deleersnyder, H. Mehdi, I.T. Horvath, K. Binnemans, T.N.P. Vogt, Tetrahedron 63 (2007) 9063.

[5] Z.H. Abd El-Wahab, M.M. Mashaly, A.A. Salman, B.A. El-Shetary, A.A. Faheim, Spectrochim. Acta Part A 60 (2004) 2861.
[6] M.M. Mashaly, Z.H. Abd El-Wahab, A.A. Faheim, Synth. React. Inorg. Met.-Org. Chem. 34 (2004) 233.
[7] Z.H. Abd El-Wahab, M.M. Mashaly, A.A. Faheim, Chem. Pap. 59 (2005) 25.
[8] M.M. Mashaly, Z.H. Abd El-Wahab, A.A. Faheim, J. Chin. Chem. Soc. 51 (2004) 901.
[9] K. Edwards, S.N. Herringer, A.R. Parent, M. Provost, K.C. Shortsleeves, M.M. Turnbull, L.N. Dawe, Inorg. Chim. Acta 368 (2011) 141.
[10] C. Yenikaya, M. Poyraz, M. San, F. Demirci, H. Ilkimen, O. Buyukgungor, Polyhedron 28 (2009) 3526.
[11] S.P. Jose, S. Mohan, Spectrochim. Acta Part A 64 (2006) 240.
[12] C. Yenikaya, M. Sari, M. Bulbul, H. Ilkimen, H. Celik, O. Buyukgungor, Bioorg. Med. Chem. 18 (2010) 930.
[13] R. Yesilagac, P. Unak, E.I. Medine, C.A. Ichedef, T. Ertay, F.Z.B. Muftuler, Appl. Radiat. Isot. 69 (2011) 299.
[14] H.P. Zeng, T.T. Wang, X.H. Ouyang, Y.D. Zhou, H.L. Jing, G.Z. Yuan, D.F. Chen, S.H. Du, H. Li, J.H. Zhou, Bioorg. Med. Chem. 14 (2006) 5446.
[15] K. Arıcı, M. Yurdakul, S. Yurdakul, Spectrochim. Acta Part A 61 (2005) 37.
[16] R. Mladenova, M. Ignatova, N. Manolova, T. Petrova, I. Rashkov, Eur. Polym. J. 38 (2002) 989.
[17] A.A. Ibrahim, A.M. Adel, Z.H. Abd El-Wahab, M.T. Al-Shemy, Carbohydr. Polym. 83 (2011) 94.
[18] M. Shebl, S.M.E. Khalil, F.S. Al-Gohani, J. Mol. Struct. 980 (2010) 78.
[19] K. Singh, Y. Kumar, P. Puri, M. Kumar, C. Sharma, Eur. J. Med. Chem. 52 (2012) 313.
[20] S.A. Khan, M. Yusuf, Eur. J. Med. Chem. 44 (2009) 2597.
[21] K.V. Sharma, V. Sharma, U.N. Tripathai, J. Coord. Chem. 62 (2009) 676.
[22] E. Erdem, E.Y. Sari, R. Kilincarslan, N. Kabay, Transition Met. Chem. 34 (2009) 167.
[23] S.J. Peng, L.B. Song, J.H. Ning, Z.L. Xiao, Synth. React. Inorg. Met.-Org. Nano-Met. Chem. 40 (2010) 105.
[24] M. Shebl, S.M.E. Khalil, S.A. Ahmed, H.A.A. Medien, J. Mol. Struct. 980 (2010) 39.
[25] A. Manimaran, C. Jayabalakrishnan, Synth. React. Inorg. Met-Org.Nano- Met. Chem. 40 (2010) 116.
[26] Z.H. Abd El-Wahab, J. Coord. Chem. 61 (2008) 1696.
[27] A. Sui, X. Xu, Z. Tang, F. Wen, J. Coord. Chem. 61 (2008) 2760.
[28] A.C.G. Hotze, H. Kooijman, A.L. Spek, J.G. Haasnoot, J. Reedijk, New. J. Chem. 28 (2004) 565.
[29] M. Shakir, A. Abbasi, A.U. Khan, S.N. Khan, Spectrochim. Acta Part A 78 (2011) 29.
[30] S. Ramalingam, S. Periandy, B. Elanchezhian, S. Mohan, Spectrochim. Acta Part A 78 (2011) 429.
[31] Y. Yang, S. Mu, Electrochim. Acta 54 (2008) 506.
[32] S.A. Patil, S.N. Unki, A.D. Kulkarni, V.H. Naik, P.S. Badami, J. Mol. Struct. 985 (2011) 330.
[33] M.A. Diab, A.A. El-Bindary, A.Z. El-Sonbati, O.L. Salem, J. Mol. Struct. 1007 (2012) 11.
[34] A.R. Fakhari, A.R. Khorrami, H. Naeimi, Talanta 66 (2005) 813.
[35] A.D. Khalaji, S.M. Rad, G. Grivani, D. Das, J. Therm. Anal. Calorim. 103 (2011) 747.
[36] A.A.A. Abou-Hussen, J. Sulfur Chem. 31 (2010) 427.
[37] A.K. Sharma, S. Chandra, Spectrochim. Acta Part A78 (2011) 337.
[38] A.A. Nejo, G.A. Kolawole, A.O. Nejo, J. Coord. Chem. 63 (2010) 4398.
[39] A.A. El-Sherif, T.M.A. Eldebss, Spectrochim. Acta Part A 79 (2011) 1803.
[40] C. Yenikaya, M. Sarl, H. Ilkimen, M. Bulbul, O. Buyukgungor, Polyhedron 30 (2011) 535.
[41] J.F. Wang, N. Ren, F.T. Meng, J.J. Zhang, Thermochim. Acta 512 (2011) 118.
[42] T. Rosu, E. Pahontu, M.R. Stefana, D.C. Ilies, R. Georgescu, S. Shova, A. Gulea, Polyhedron 31 (2012) 352.
[43] Z.H. Abd El-Wahab, J. Coord. Chem. 61 (2008) 3284.
[44] N.J. Parmar, S.B. Teraiya, R.A. Patel, J. Coord. Chem. 63 (2010) 3279.
[45] B. Samanta, J. Chakraborty, S. Shit, S.R. Batten, P. Jensen, J.D. Masuda, S. Mitra, Inorg. Chim. Acta 360 (2007) 2471.
[46] T.A. Yousef, T.H. Rakha, U. El Ayaan, G.M. Abu El Reash, J. Mol. Struct. 1007 (2012) 146.
[47] R.N. Patel, A. Singh, K.K. Shukla, D.K. Patel, V.P. Sondhiya, Transition Met. Chem. 36 (2011) 179.
[48] M.M.H. Khalil, M.M. Mashaly, Chin. J. Chem. 26 (2008) 1669.
[49] M. Shakir, H.T.N. Chishti, P. Chingsubam, Spectrochim. Acta Part A 64 (2006) 512.
[50] H. Unver, Z. Hayvali, Spectrochim. Acta Part A 75 (2010) 782.
[51] O.M.I. Adly, Spectrochim. Acta Part A 79 (2011) 1295.
[52] M.M. Mashaly, Synth. React. Inorg. Met.-Org. Chem. 32 (2002) 373.
[53] M. Arshad, A.H. Qureshi, S. Rehman, K. Masud, J. Therm. Anal. Calorim. 89 (2007) 561.
[54] J.F. Wang, F.T. Meng, S.L. Xu, X. Liu, J.J. Zhang, Thermochim. Acta 521 (2011) 2.
[55] B.P. Baranwa, T. Fatma, A. Varma, A.K. Singh, Spectrochim. Acta Part A 75 (2010) 1177.
[56] B.P. Baranwa, T. Fatma, A. Varma, J. Mol. Struct. 920 (2009) 472.
[57] V. Singh, P. Gupta, J. Coord. Chem. 59 (2006) 1483.
[58] R.R. Zaky, K.M. Ibrahim, I.M. Gabr, Spectrochim. Acta Part A 81 (2011) 28.
[59] M. Zaheer, A. Shah, Z. Akhter, R. Qureshi, B. Mirza, M. Tauseef, M. Boltec, Appl. Organometal. Chem. 25 (2011) 61.
[60] G.S. Kurdekar, S.M. Puttanagouda, N.V. Kulkarni, S. Budagumpi, V.K. Revankar, Med. Chem. Res. 20 (2011) 421.
[61] M.N. Patel, M.R. Chhasatia, P.A. Dosi, H.S. Bariya, V.R. Thakkar, Polyhedron 29 (2010) 1918.
[62] J. Bassett, R.C. Denney, G.H. Jeffery, J. Mendham, Vogel's Textbook of Quantitative Inorganic Analysis, fourth ed., Longmans, London, 1978.